EXPERIMENTAL AND THEORETICAL STUDIES OF THE TEMPERATURE RAMPED SCREENING TEST FOR THE THERMAL STABILITY OF POWDERS

X. Z. Wan[1], J. S. Hardman[1], D. J. Harper[2], T. G. Nevell[1]* and R. L. Rogers[2]
[1]Department of Chemistry, University of Portsmouth, Portsmouth, PO1 2DT
[2]Zeneca Fine Chemicals Manufacturing Organisation, Blackley, Manchester, M9 3DA.

The behaviour of unstable solids and activated carbon has been studied in temperature-ramped tests carried out with static air and preheated flowing air. Measured temperature distributions (central diameter and vertical axis of cylindrical samples) show appreciable temperature gradients, influenced by factors including thermal conductivity and packing density. Exothermic reactions are first detectable at the bed centre, where temperatures rise most rapidly for combustion under static air and for decomposition. For combustion with flowing air, the "hot spot" progresses towards the source of air. Temperature changes during early stages of combustion have been modelled.

Key Words: thermal stability, powders

INTRODUCTION

Several small-scale (50 - 200g) tests are in use for screening potentially combustible materials or unstable materials to establish maximum safe temperatures for their transportation and storage in bulk quantities. These include the temperature-ramped thermal stability test developed by Gibson *et al* (1) at ICI. Such tests are much less time-consuming and require much smaller samples than standard isothermal tests. Although the adequacy of small-scale tests has been established by their use over several years, it is clearly desirable to establish a link between the results of small-scale tests and those for the standard isothermal tests. As the first stage in this exercise the behaviour of unstable and combustible materials in the ICI test has been investigated.

In the ICI test, a sample of powder (118 cm^3) in a cylindrical vessel with a sintered glass base, Figure 1, is heated at 0.5 K min^{-1}. Temperatures are monitored continuously at several points within the sample. The onset temperature for an exothermic reaction in the sample is taken as the sample temperature at which any one of the monitored temperatures starts to rise at 0.6 K min^{-1}. The test may be carried out under static air using an open-topped vessel, or with pre-heated air passed downwards through the sample bed.

In this study, temperature distributions have been measured along horizontal and vertical axes in samples of unstable and combustible materials (respectively, two synthetic dyestuffs and activated carbon) subjected to the ICI test. The effect of flowing air has been measured, and the finite element method has been used to calculate temperature distributions within samples of solids liable to undergo exothermic reaction, heated at a constant rate.

EXPERIMENTAL

Test cells

Cylindrical borosilicate glass vessels were used, with thermocouples located on horizontal or vertical axes, Figure 1. When required, preheated air was passed downwards through the sample via a lid fitted to the cell with a flange joint. The chromel-alumel thermocouples (0.2 mm glass fibre insulated extension cables type K, TC Ltd Uxbridge) were calibrated at 0°C and 100°C and were monitored using a potentiometric recorder (Chessel 320) or a temperature scanner mutiplexer unit (CRL 620) interfaced with a microcomputer.

Materials

α-Alumina, calcium carbonate and titania, ("Analar") and dyestuffs "A" and "B" (Zeneca Fine Chemicals Manufacturing Organisation) were sieved to 80-120 mesh. Activated carbon type 207B (Sutcliffe Speakman Ltd) was ground and sieved to 12-14 mesh and 300-350 mesh.

Differential thermal analysis (DTA), Figure 2, showed that dyestuffs A and B each decomposed exothermically in a single stage which was preceded by a much smaller endotherm. Above a critical heating rate (9 K min^{-1} for A and 4 K min^{-1} for B) onset temperatures were increased and the peaks became extremely sharp. Enthalpies of decomposition were estimated (+/- 40 J g^{-1}) as A, -1900 J g^{-1} and B, -850 J g^{-1}. Very similar results were obtained under static air and under flowing nitrogen. Under static air, activated carbon was oxidised at above 285°C in DTA experiments. Isothermal basket tests, Beever (2), in sizes 100 cm^3 to 1000 cm^3 gave an activation energy of 114 kJ mol^{-1}.

Calculations

Finite element calculations were performed using parts of the Berkeley Structural Analysis by Finite Elements (BERSAFE) package, Keavey (3), run on a Vax 6310 computer. A cylindrical body of unstable material was treated as an assembly of 200 elements (five layers each of 40). For each element, linear energy balance equations were set up using the Crank-Nicholson method, Myers (4). The heat capacity and thermal conductivity of the material were required, together with the rate of heat generation per unit volume (as a function of temperature) and the convective heat transfer coefficient of the surface. Radiation was not included.

RESULTS

Inert materials

α-Alumina, calcium carbonate and titania were heated in test cells at constant rates in the range 0.3 K min^{-1} to 5.0 K min^{-1}, Figure 3. Constant profiles of temperature across the beds were established after the oven temperature (T_6) had risen by ca. 50 K at 0.5 K min^{-1} but by rather more at higher heating rates. Temperature differences between the edge (T_1) and the centre (T_3) of the bed were less than 5 K for α-alumina at lower heating rates but approached 80 K for calcium

carbonate and titania at 5 K min^{-1}. The difference (T_1-T_3) was proportional to heating rate and correlated approximately with the thermal conductivity of the material. Beds of the larger carbon particles gave smaller temperature differences. Temperature gradients across the glass wall of the cell were considerable at high heating rates.

Dyestuffs A and B

Temperatures at points on a central diameter during temperature-ramped experiments using the ICI cell are shown in Figures 4 and 5 as (a) horizontal temperature profiles at selected times and (b) plots of temperature against time for individual thermocouples. With both dyestuffs, considerable temperature gradients were generated at early stages between the edge and centre of the bed (T_1-T_3) and across the glass (T_6-T_1). These differences were similar for the two substances. Self-heating then started in the centre of the bed so that, as the ambient temperature was raised, the profile flattened progressively and became inverted. Then with dyestuff A an extremely rapid reaction was recorded, starting close to the centre and spreading across the cell. With dyestuff B the major rise in temperature was smaller and more uniformly distributed. In both cases heat was evolved so rapidly that the temperature recorded at 10 mm from the cell wall was higher than the programmed value (beyond points X in Figures 4b, 5b). From readings of the central thermocouple (T_3) the difference between the onset of the exotherm and the very rapid reaction was ca. 90 K for A and ca. 35 K for B. Correspondingly, if the onset temperature is taken as the oven temperature (T_6) at which exothermic reaction becomes detectable, the results from central (T_3) and edge (T_1) thermocouples are much more similar for dyestuff B than for dyestuff A.

The effects of passing air through a cell containing dyestuff B are shown in Figure 6. Before the onset of decomposition in ramped experiments, temperature differences (T_6-T_1) and (T_1-T_3) in horizontal profiles were considerably reduced, ie the flow of preheated air reduced temperature gradients both across the glass wall and within the bed . Along the central vertical axis temperature gradients were also small, and both vertical and horizontal measurements showed that exothermic decomposition started close to the centre of the bed. Very similar onset temperatures (T_6) were obtained with reference to all thermocouples and the rapid decomposition stage was reasonably uniform throughout the bed. The onset temperature was 170±/2°C at all flow rates in the range 0-1500 cm^3 min^{-1}.

Activated carbon

Under static air, Figure 7, a characteristic horizontal temperature distribution was obtained at low temperatures ((T_1-T_3) ca. 8 K at 0.5 K min^{-1}) and the internal thermocouples registered an accelerating exothermic process above ca. 210°C. However, no very rapid evolution of heat was observed, the maximum temperature difference (T_3-T_6) being ca. 40 K. Consequently, the onset temperature was difficult to determine precisely. Between 65% and 85% of carbon remained unburnt after samples were allowed to cool from ca. 400°C.

Under flowing air, Figure 8, exothermic reaction did not become apparent until a much higher temperature had been reached, but the subsequent acceleration was

more rapid. The vertical temperature profiles, Figure 8c, show that combustion commenced in the centre of the bed, but the location of the maximum temperature was subsequently displaced upwards towards the source of air. Between 50% and 75% of carbon remained unburnt after tests.

Calculations

Since kinetic data are not available for dyestuffs A and B, preliminary calculations have been performed for the combustion of carbon. It has been assumed that, at temperatures close to the onset of combustion, the availability of air does not limit the reaction rate. The rate of evolution of heat (dQ/dt) is given by

$$dQ/dt = \Delta H\ p\ S\ A\ e^{-E/RT} \qquad (1)$$

where p is the ambient pressure of oxygen over surface area S, A and E are kinetic parameters and ΔH is the heat of combustion. Assuming that particles (20 μ) are burnt to carbon dioxide ($\Delta H = 3.31 \times 10^7$ J kg^{-1}), using the parameters,

$A = 8710$ g cm^{-2} s^{-1} atm^{-1}
$E = 1.49 \times 10^8$ J kmol^{-1} (149 kJ mol^{-1}),

Field *et al* (5), and taking into account a typical packing density of 0.55 g cm^{-3},

$$(dQ/dt)_1 = 5.0 \times 10^{10} e^{-17966/T} \text{ J mm}^{-3} \text{ s}^{-1} \qquad (2)$$

The inclusion of data from equation (2) in the finite element calculation of the temperature distribution in a bed of carbon particles heated at 0.5 K min^{-1} led to realistic profiles when combustion was insignificant, but also to a prediction that the temperature at the centre of the bed would rise extremely rapidly when reaction commenced. This prediction, which did not correspond with observation, was associated mainly with the high value of the activation energy, E. Alternatively,

$$(dQ/dt)_2 = 15.7e^{-9000/T} \text{ J mm}^{-3} \text{ s}^{-1} \qquad (3)$$

which includes the activation energy of 74.85 kJ mol^{-1} for the chemisorption of molecular oxygen on carbon, Karsner and Perlmutter (6), and an arbitrary pre-exponential factor. A comparison between observed and calculated horizontal temperature profiles, Figure 9, shows good agreement from low ambient temperature to just above the onset temperature, but therafter the calculated difference (T_1-T_3) still rises somewhat more rapidly than was observed.

DISCUSSION

Temperature profiles in the absence of reaction for inert materials and for reactive materials at low temperatures, show that considerable temperature gradients are generated both within the materials in the cell and across the glass wall, even at heating rates as low as 0.5 K min^{-1}. Temperature gradients are determined by the thermal conductivity and by the heat capacity per unit volume, which is related to packing density and hence to particle size.

Since in all temperature-ramped experiments using the test cell, with or without flowing air, the onset of exothermic reaction was detected at the centre of the cell, removal of heat by flowing air was not significant. With the exothermic decompositions of A and B, as the ambient temperature was increased, the highest temperature remained in the centre of the cell until the very rapid reaction occurred. Onset temperatures were 30-50 K lower in the ICI test than in DTA experiments. These differences are appreciable, but not as large as that reported previously for the unstable material, zoalene, HM Factory Inspectorate (7).

The combustion of carbon was observed to accelerate over an extended range of temperature showing that the overall activation energy was relatively low. The reaction involves, sequentially, gas-phase and pore diffusion of oxygen, chemisorption and reaction, and diffusion of the gaseous combustion products. The rate is probably influenced by diffusion in pores, which would reduce the overall activation energy, Satterfield (8). However, since the calculated acceleration in heat generation with increasing temperature was too great even when the lower activation energy was used, the consumption of oxygen also must be a major factor.

In conclusion, the experiments have established qualitatively the temperature gradients and profiles which are developed when an unstable or combustible powder is subjected to the ICI temperature-ramped thermal stability test. The calculation of such profiles by the finite element method has been shown to be practicable, and this will be developed for larger samples of unstable material.

REFERENCES

1. N. Gibson, D. J. Harper and R. L. Rogers, 1985, Plant/Operations Progress 4(3), 181.

2. P. F. Beever, 1980, I. Chem. E. Symposium Series no. 68, 4/X:1.

3. M. A. Keavey, 1982, "A User's Guide to FLHE Level 2" Berkeley Nuclear Laboratories.

4. G. E. Myers, 1971, "Analytical Methods in Conduction Heat Transfer" McGraw Hill.

5. M. A. Field, D. W. Gill, B. B. Morgan and P. G. W. Hawksley, 1967, "Combustion of Pulverised Coal" British Coal Utilisation Research Association, Leatherhead.

6. G. G. Karsner and D. D. Perlmutter, 1982, Fuel 61, 35.

7. H. M. Factory Inspectorate, 1977, "The Explosion at the Dow Chemicals Factory, Kings Lynn, June 27 1976" Health and Safety Executive HMSO, London.

8. C. N. Satterfield, 1970, "Mass Transfer in Heterogeneous Catalysis" M.I.T. Press, Cambridge Ma.

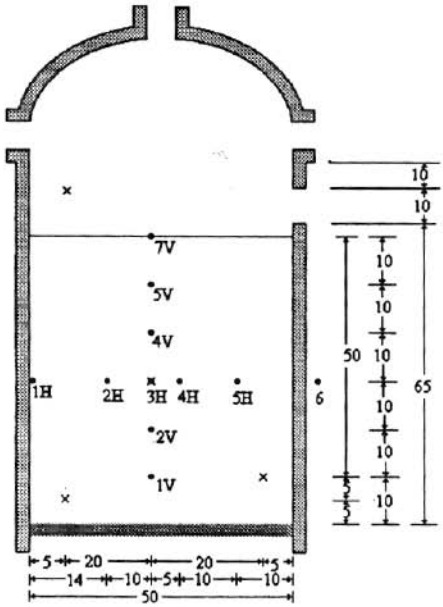

Figure 1. Test cell; thermocouples: in Zeneca tests X, horizontal diameter .H, vertical axis .V; dimensions in millimetres.

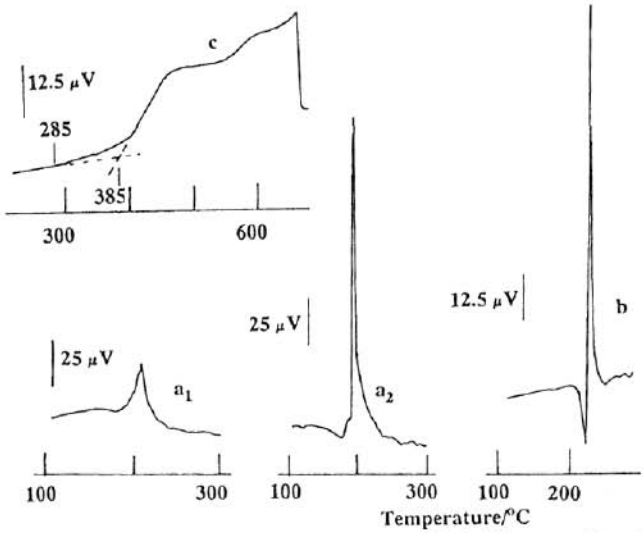

Figure 2. Differential thermal analysis: dyestuff A (40 mg under air or nitrogen, a_1 8 K min^{-1}, a_2 10 K min^{-1}), dyestuff B (b, 40 mg under air or nitrogen, 5 K min^{-1}), activated carbon 300-350 mesh (c, 40 mg under air, 1 K min^{-1}).

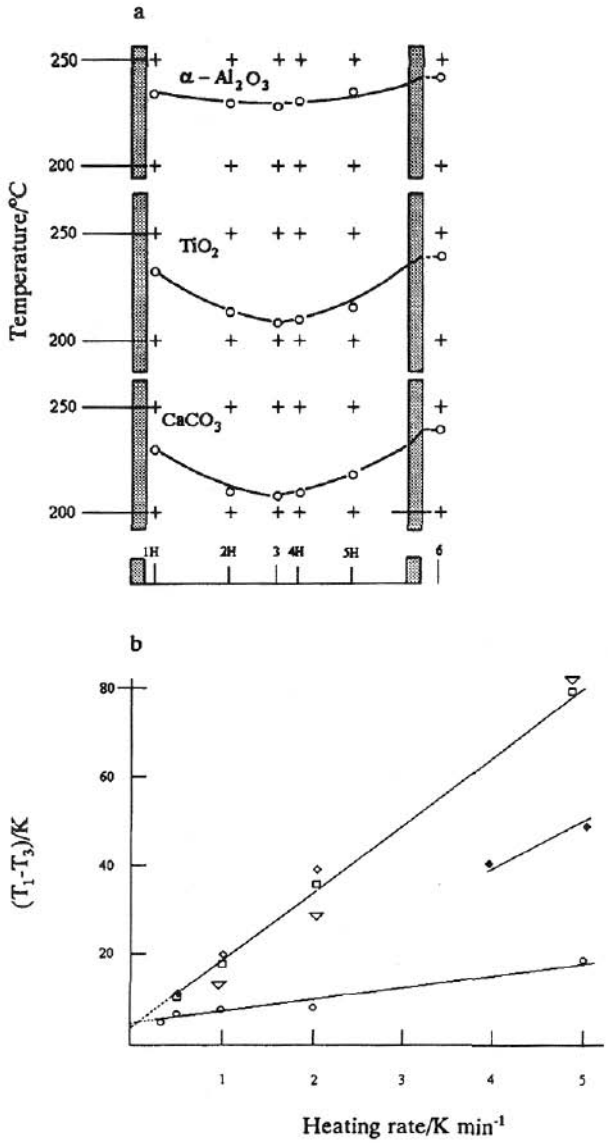

Figure 3. Inert powders heated in the test cell under static air: (a) horizontal temperature profiles, heating rate 1.0 K min^{-1}; (b) temperature gradients (T_1-T_3) for α-alumina ○, calcium carbonate □, carbon 12-14 mesh ◇, carbon 300-350 mesh ◆, titania ▽, at various heating rates.

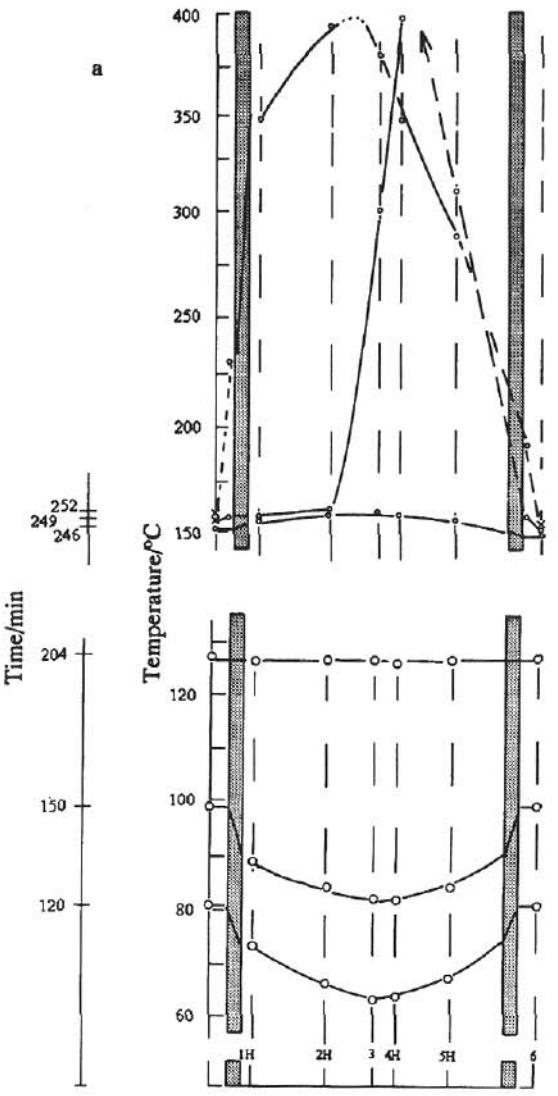

Figure 4. Dyestuff A heated in the test cell at 0.5 K min^{-1} under static air: (a) horizontal temperature profiles, (b) temperatures inside the wall T_{H1}, at the centre T_3, outside the cell T_6.

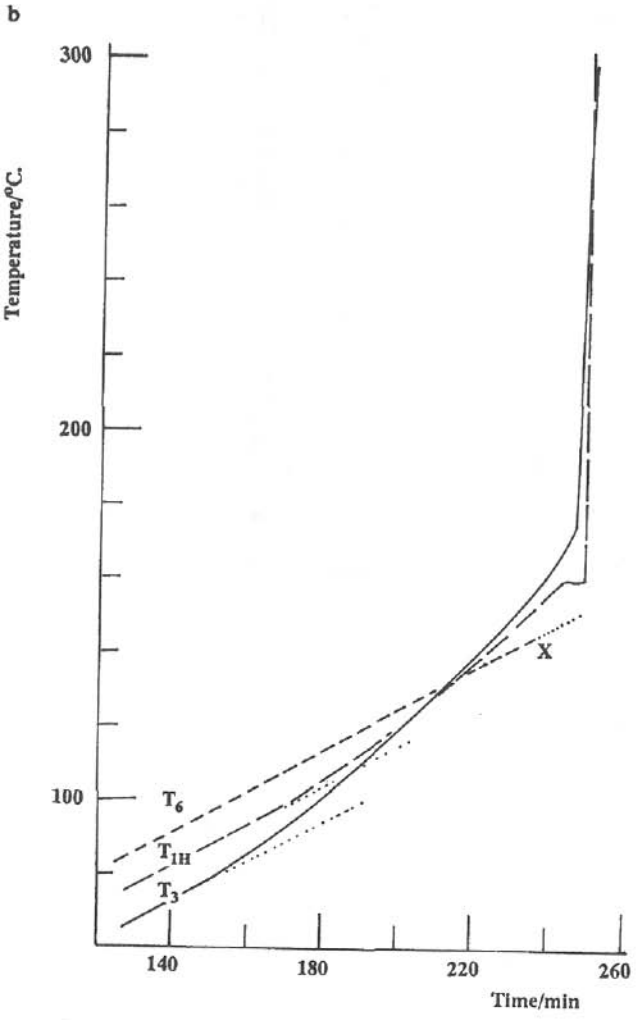
b
300
200
100
Temperature/°C.
T_6
T_{1H}
T_3
X
140
180
220
260
Time/min

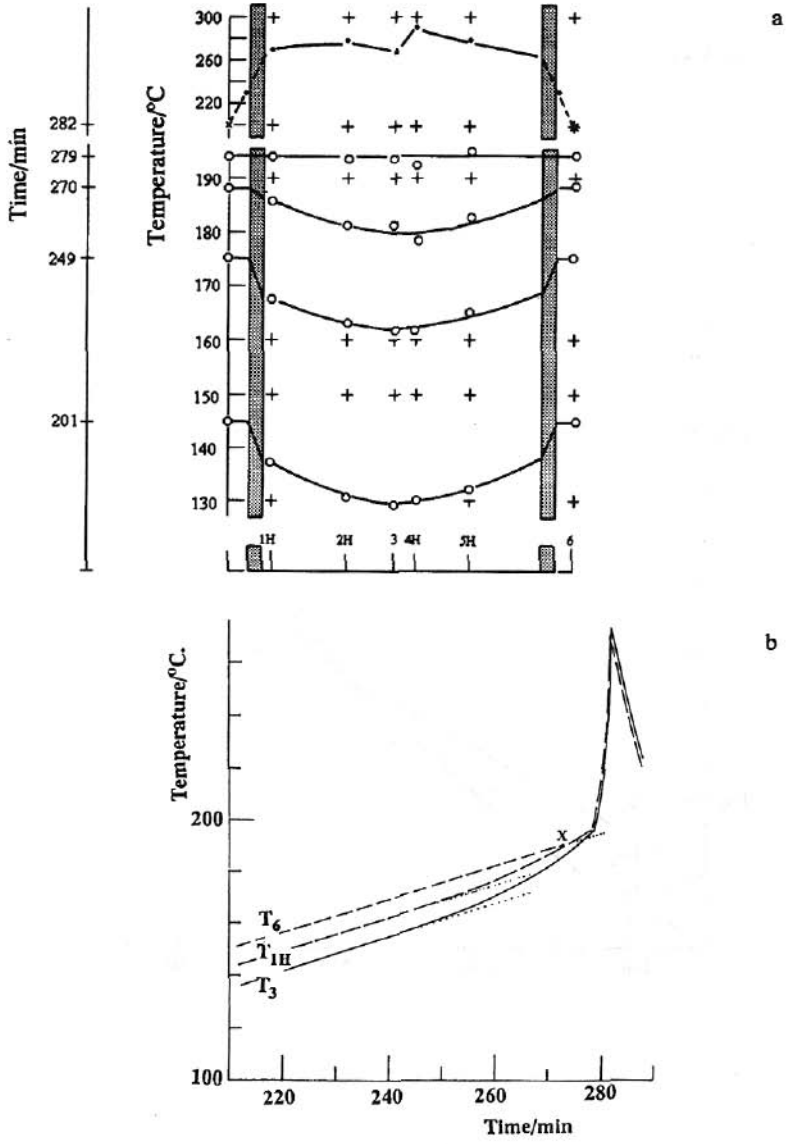

Figure 5. Dyestuff B heated in the test cell at 0.5 K min^{-1} under static air: (a) horizontal temperature profiles, (b) temperatures inside the wall T_{H1}, at the centre T_3, outside the cell T_6.

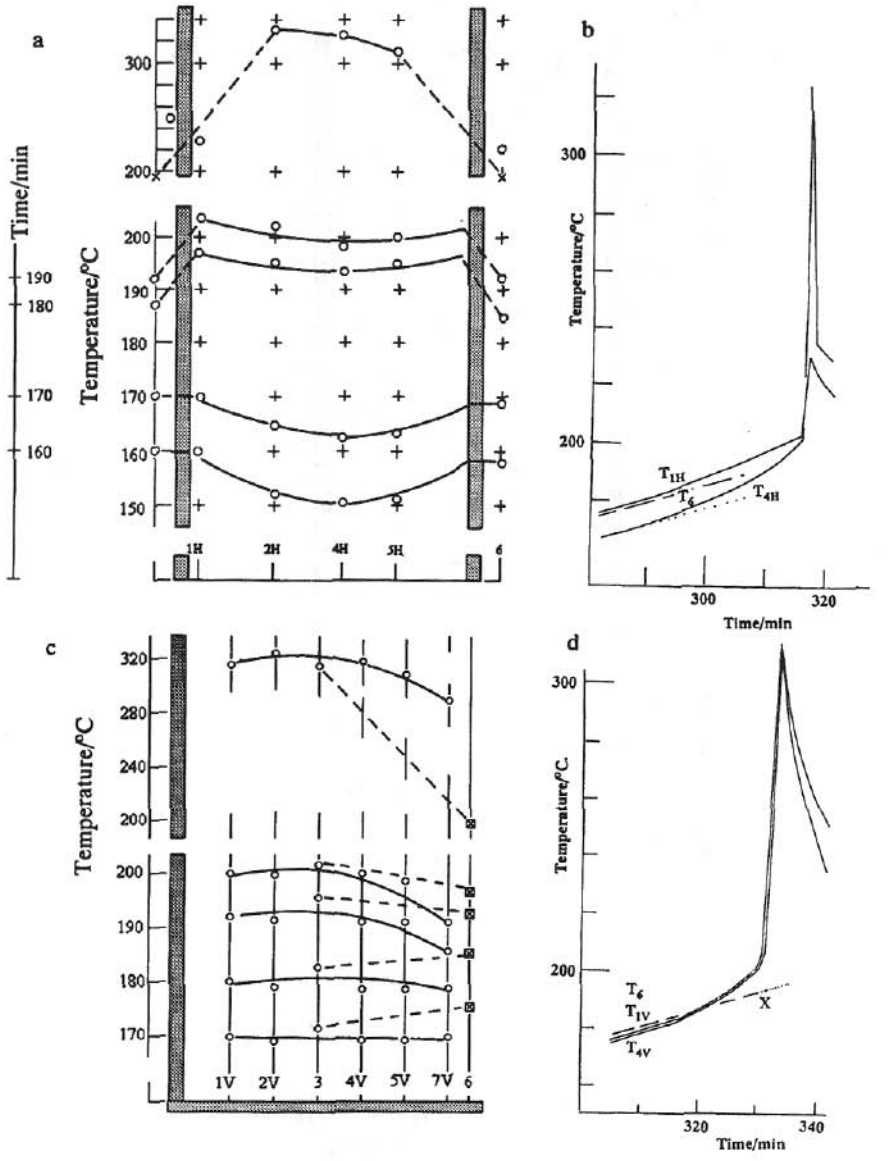

Figure 6. Dyestuff B heated at 0.5 K min^{-1} under flowing air (1000 cm^3 min^{-1}): (a) horizontal temperature profiles, (b) and (d) temperatures inside the wall T_{H1}, at the centre T_{4H}, above and below the centre T_{4V} and T_{1V}, outside the cell T_6; (c) vertical temperature profiles.

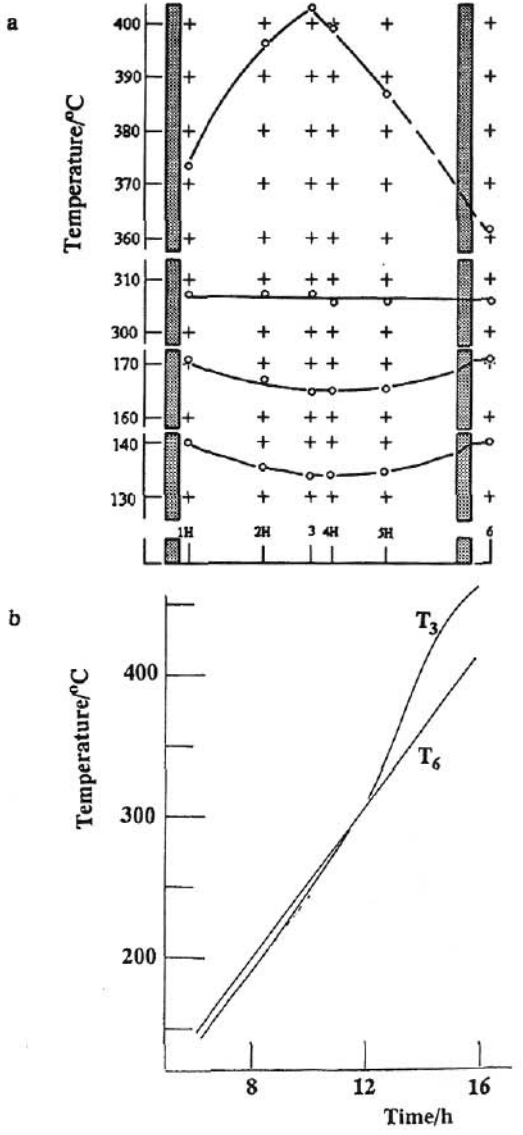

Figure 7. Activated carbon heated in the test cell at 0.5 K min^{-1} under static air: (a) horizontal temperature profiles; (b) centre temperature T_3 and oven temperature T_6.

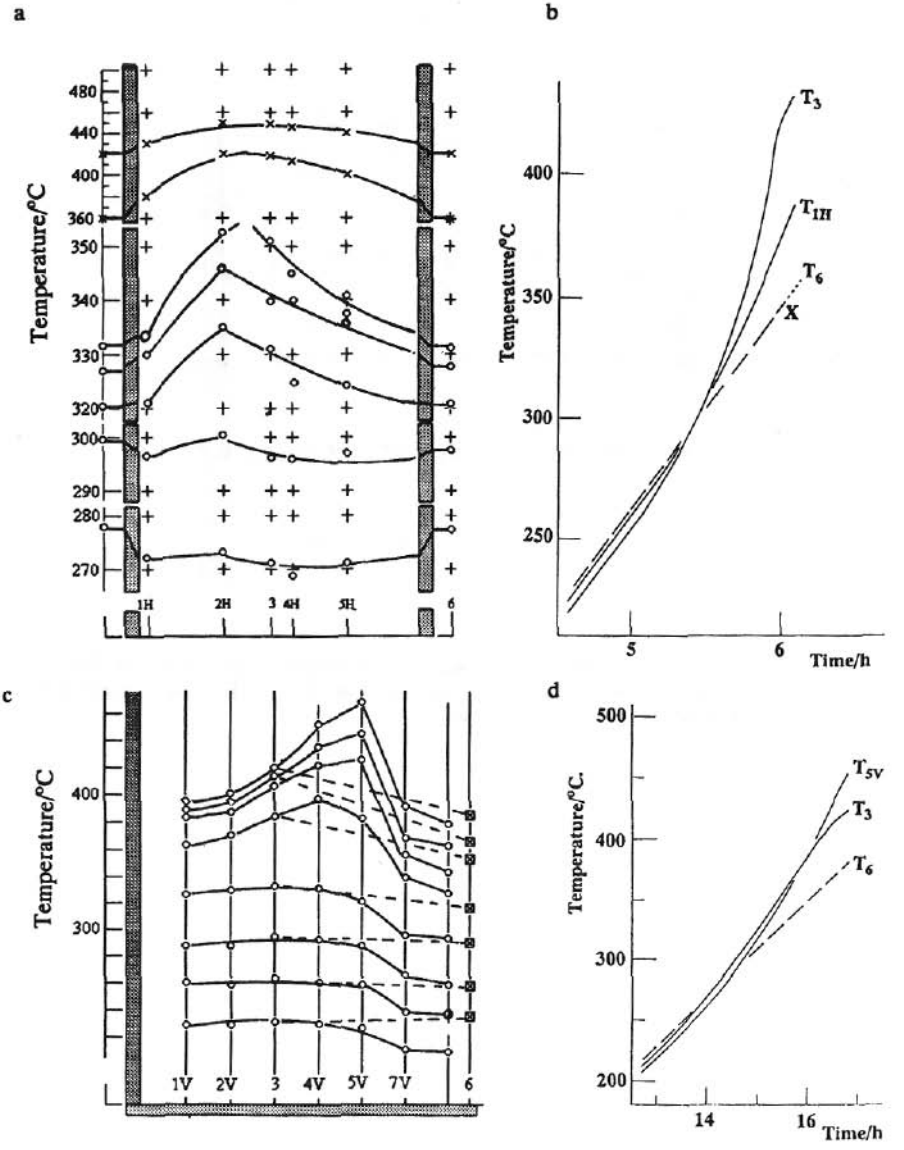

Figure 8. Activated carbon heated in the test cell under flowing air: (a) and (b) horizontal temperature profiles (flow rate 5000 cm^3 min^{-1}, heating rate 1.0 K min^{-1}); (c) and (d) vertical temperature profiles (flow rate 1900 cm^3 min^{-1}, heating rate 1.0 K min^{-1}).

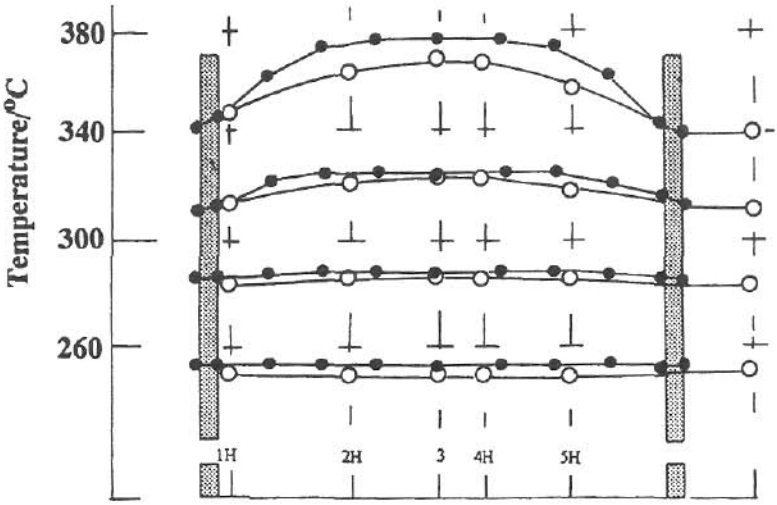

Figure 9. Comparison of observed and calculated horizontal temperature profiles for activated carbon heated in the test cell at 0.5 K min^{-1} under air: observations O, calculations ● .